# GLOBAL SCALE IONOSPHERIC IRREGULARITIES ASSOCIATED WITH THUNDERSTORM ACTIVITY

**Sergey A. Pulinets[1] and Victor H. Depuev[2]**

[1]*Instituto de Geofísica, UNAM, Ciudad Universitaria, Delegación de Coyoacán, 04510, México D.F., México*
[2]*Institute of Terrestrial Magnetism, Ionosphere and Radiowave Propagation, RAS, (IZMIRAN), Troitsk, Moscow Region, 142190, Russia*

**Abstract:** The potential difference near 280 kV exists between ground and ionosphere. This potential difference is generated by thunderstorm discharges all over the world, and return current closes the circuit in the areas of fair weather (so-called fair weather current). The model calculations and experimental measurements clearly demonstrate non-uniform latitude-longitude distribution of electric field within the atmosphere. The recent calculations show that the strong large scale vertical atmospheric electric field can penetrate into the ionosphere and create large scale irregularities of the electron concentration. To check this the global distributions of thunderstorm activity obtained with the satellite monitoring for different seasons were compared with the global distributions of ionosphere critical frequency (which is equivalent to peak electron concentration) obtained with the help of satellite topside sounding. The similarity of the obtained global distributions clearly demonstrates the effects of thunderstorm electric fields onto the Earth's ionosphere.

## Introduction

The global electric circuit concept is now widely accepted. The most recent publication describing the mechanism of atmospheric electric field generation one can find in [*Bering et al.,* 1998]. More deep and detailed review including the model calculations of the global distribution of atmospheric electric field on different heights is given in [*Roble and Tzur,* 1986]. Thunderstorms supply to the Earth the negative charge creating the current of about 1.7 A per thunderstorm cell in average. The positive charge is transferred to the upper atmosphere which conductivity growths with the altitude. All thunderstorms together all over the world provide the potential difference between the ground and ionosphere several hundred thousand volts with the mean value near 280 kV. This potential difference should create the return current from the ionosphere to the ground which is measured experimentally in the fair weather areas and makes $(1 \div 2.5) \cdot 10^{-12}$ A.

*Park and Dejnakarintra* [1973, 1977] calculated the penetration of electric field from the thunderstorm cloud into the ionosphere in approximation of vertical geomagnetic field lines and obtained value of order $10^{-4}$ V/m of the electric field perpendicular to the geomagnetic field lines within the ionosphere at 100 km altitude. *Kim and Khegai* [1985] and *Hegai and Kim* [1990] modified the boundary conditions for the Park and Dejnakarintra's approach. Their calculations improved the effectiveness of electric field penetration into ionosphere by one order coming to the value of 1 mV/m. As Park and Dejnakarintra, so Kim and Hegai demonstrated that effectiveness of electric field penetration into the ionosphere by 1-2 orders higher for nighttime conditions because of increased ionospheric electrical conductivity during daytime.

*Pulinets et al.* [1998, 2000] demonstrated by model calculations and experimentally the effects of the large scale atmospheric electric field of different origin onto the ionosphere at different heights including effects on E and F-regions of the ionosphere. But these results relate to localized irregularities of electron concentration within the ionosphere associated with the local sources of anomalous electric field. The individual thunderstorm cloud is also the localized source of the electric field of large magnitude, but having in mind the non-uniform distribution of thunderstorm activity over the globe it is worth to make study of its global scale effects on the ionosphere, what is the purpose of the present paper.

**Data sources**

There are no too much sources of experimental measurements providing enough data to built the maps of global distribution of the electron concentration within the ionosphere. The International Reference Ionosphere model (IRI) is based on empirical measurements of the global network of ground based ionosondes [*Bilitza*, 2001]. Its main deficiency lies in non-uniform distribution of data sources – ionospheric stations: no data for ocean covered areas, more stations in Northern hemisphere, more stations in Eastern hemisphere. But it is only internationally accepted model based on empirical data. For the peak values of the ionosphere the model provides the set of coefficients representing the spherical deconvolution of experimental data fit (monthly medians), so called CCIR coefficients [*CCIR (International Radio...*, 1991].

The second data source – is the data from satellite sounding of the ionosphere, called topside sounding. There were a number of topside sounding satellites [*Pulinets,* 1989], but only two of them – Russian Intercosmos-19 and Japanese ISS-B satellites provided the data enough to build the global maps of electron concentration within the ionosphere. The advantages of the topside sounding technique are described in [*Pulinets and Benson*, 1999], but the main advantage is that satellite provides the uniform grid of data points including ocean covered areas, and therefore the satellite maps are more adequate than that of the IRI model. Except

published catalogues [*Atlas of Ionospheric...*, 1979] the Japanese data are practically unreachable, so we used the data of Intercosmos-19 satellite, which were reprocessed and accomplished within the frame of NASA grant NRA 98-OSS-03(5.2) "Intercosmos-19 topside sounder data rescue project" [*http://antares.izmiran.rssi.ru/projects/IK19/*]. Unfortunately, the Intercosmos-19 lifetime (March 1979 – July 1981) is very far from the times when the real-time satellite monitoring (Optical Transient Detector) of the thunderstorm activity data became available [*http://thunder.nsstc.nasa.gov/data/OTDsummaries/ (Optical Transient Detector)*]. So for comparison the same months (July and November) and the similar levels of the solar activity were selected. The last is very important because of essential dependence of ionospheric parameters on the solar activity within the 11-year solar cycle provided by changes of solar ultraviolet radiation ionising the ionosphere [*Science of Space Environment*, 2000]. It was detected recently the dependence of thunderstorm activity on the solar activity also [*Schlegel et al.*, 2001]. Close values of the solar spot number were selected to provide the similar ambient conditions for the both sets of experimental data. The data selected are presented in Table 1

**Table 1.**

| Intercosmos-19 | | Optical Transient Detector | |
|---|---|---|---|
| Month, year | W | Month, year | W |
| July, 1980 | 136.3 | July, 1999 | 113.5 |
| November, 1980 | 147.9 | November, 1999 | 133.2 |

**LT map conception**

The Earth's ionosphere is very dynamic medium. Driven mainly by the solar activity, it contains many kinds of variability of different temporal and spatial scales. The most pronounced in amplitude is the daily variability because the most part of ionisation within the ionosphere is provided by solar ultraviolet radiation during daytime. The difference between the daytime and nighttime values of the electron concentration can reach two orders of magnitude. Minimal value of electron concentration within the ionosphere is observed before sunrise (between 02 h and 05 h of local time LT, depending on concrete place and season). To exclude the daily variations within the ionosphere the conception of fixed local time map was put forward. It is artificial map using the same local time all over the globe, so called LT map. Such map is excellent means to reveal the longitude variations within the ionosphere, i.e. to see how different is ionosphere on different longitudes for the same geophysical conditions including the local time [*Depuev and Pulinets*, 2001]. The orbit configuration of high inclination satellite gives opportunity during the short period (near 24 hours) to collect information sufficient to produce the global map for the fixed local time. The two consecutive days of the satellite monitoring produce more dense grid for the map construction. Intercosmos-

19 satellite orbit was in pre-sunrise position (near 5 h LT), when the minimal residuals of solar influence onto the ionosphere could be expected, in July and November of 1980. So these periods were selected for map construction and for comparison. In addition it should be mentioned that according to statistical data of thunderstorm activity July is the month of maximum activity in the Northern hemisphere, and November – is one of the months of maximum thunderstorm activity in the Southern hemisphere.

**The model data comparison**

First we would like to present the comparison of the model (IRI CCIR coefficients [*CCIR (International Radio...*, 1991]) global LT map of the critical frequency of the ionosphere for 05 h LT, July 1980 (Fig.1, top panel), with the modeled global distribution of ionospheric potential difference along constant conductivity surface near the height 105 km [*Roble and Tzur*, 1986], Fig. 1, bottom panel. Critical frequency $f_oF2$ is the maximum frequency reflected from the ionosphere studied by radio sounding technique and it is in direct relation with the peak electron concentration of the Earth's ionosphere $N_m$[16]:

$$f_oF2 \cong 8.98 \cdot \sqrt{N_m} \qquad (1)$$

so for simplicity traditionally the peak parameters of the ionosphere are presented in terms of the critical frequency directly measured.

One can see from the comparison very remarkable thing – the break in electron concentration distribution along the longitudes which practically coincides with the change of the sign of the calculated atmospheric electric field at longitudes 160°-280°. The difference of electron concentration distribution in Northern and Southern hemispheres is connected with fact that we have summer in the Northern hemisphere, and winter – in Southern one, what is the reason of the difference provided by the seasonal morphology of the ionosphere. So we can conclude that using the LT-map approach one can find the effects of electric field global distribution within the ionosphere even from the monthly median model data.

**Experimental data comparison**

In Figs. 2 and 3 the comparison of global distributions of the electron concentration (top panels) and thunderstorm activity (bottom panels) for July and November is presented respectively. The electron concentration was measured with the help of topside sounder IS-338 installed inboard the Intercosmos-19 satellite, and thunderstorm activity was registered by Optical Transient Detector device launched by Pegasus rocket April 3, 1995, into an Earth orbit of approximately 710 kilometres altitude, with an inclination of 70 degrees [*http://thunder.nsstc.nasa.gov/data/OTDsummaries/ (Optical Transient Detector)*]. In the July

pictures one can see the increased electron concentration in the Northern hemisphere consisting of three clusters centered on longitudes 40°, 120°, and 320°. The thunderstorm activity is also concentrated in the Northern hemisphere, and also consist of three clusters. The longitudinal position of Eurasian clusters corresponds to that of ionospheric irregularities, but the American cluster is 20°-30° westward in relation to the ionospheric one. Even more striking similarity one can observe on the November graphs. Again one can observe several clusters within the ionosphere repeating the longitudinal positions of the centers of thunderstorm activity. Even the shape of distribution is similar as it is seen on the longitudinal tongue stretched from 120° to 270° in Pacific area. In November as increase of electron concentration so the increase of thunderstorm activity shifted into the Southern hemisphere because of the seasonal changes, now we have the local summer in the Southern hemisphere.

## Conclusion

Basing on theoretical calculations showing the possibility of strong electric field action onto the ionosphere the comparison of global distribution of the peak electron concentration with the global distribution of thunderstorm activity was made. The both data sets were obtained from satellites with high inclination orbit. To exclude the strong local time variations connected with the changes of solar ultraviolet radiation intensity the ionospheric maps were build for the fixed local time, pre-sunrise conditions. For the thunderstorm activity the monthly average maps were taken. The comparisons clearly demonstrate the existence of global scale irregularities within the ionosphere. Their longitudinal positions correspond to position of centers of thunderstorm activity, mainly over the continents. The latitudinal and longitudinal distribution changes with the season, showing the increase as thunderstorm activity, so the electron concentration in the local summer hemisphere. The present study opens way to better understanding of atmosphere-ionosphere coupling processes, Global electric circuit action, and day-to-day ionosphere variability.

## References

Atlas of Ionospheric Critical Frequency (foF2) obtained from Ionospheric Sounding Satellite-b Observation. Issued by Radio Research Laboratory Ministry of Posts and Telecommunications, Japan, 1979

Bering III, E. A., Few, A. A., and Benbrook, J. R. The Global Electric Circuit. *Physics Today.* **51**, No.10, 24-30, 1998

Bilitza, D. International Reference Ionosphere 2000. *Radio Science.* **36**, No. 2, 261-275, 2001

CCIR (International Radio Consultive Committee). Atlas of ionospheric characteristics. *Rep.* 340-6, Int. Telecommun. Union, Geneva, 1991

Depuev, V. H., Pulinets, S. A. Global Distribution of Night-Time F2 Peak Density (Intercosmos-19 Data). *Adv. Space Res.*, **25**, No. 1, 105-108, 2001

Hegai, V. V., Kim, V. P. The formation of a cavity in the night-time midlatitude ionospheric E-region above a thundercloud. *Planet. Space Sci.*, **38**, No.6, 703-707, 1990

http://antares.izmiran.rssi.ru/projects/IK19/

http://thunder.nsstc.nasa.gov/data/OTDsummaries/ (Optical Transient Detector)

Kim, V. P., Khegai, V. V. The Effect of an Electric Field on the Nightside E Region of the Midlatitude Ionosphere. *Geomagnetism and Aeronomy*, (English Edition Published by AGU), **25**, No. 5, 717-718, 1985

Park, C. G., Dejnakarintra, M. Penetration of thundercloud electric fields into the ionosphere and magnetosphere, 1. Middle and auroral latitudes. *J. Geophys. Res.*, **84**, 960-964, 1973

Park, C. G., Dejnakarintra, M. Thundercloud electric fields in the ionosphere, in Electrical Processes in Atmospheres, Dolezhalek, H.and Reiter, R., eds., Steinkopff, Darmstadt, 544-551, 1977

Pulinets, S. A. Prospects of Topside Sounding. in *WITS handbook* N2, Chapter 3, SCOSTEP Publishing, Urbana, Illinois, 99-127, 1989

Pulinets, S. A., Khegai, V. V., Boyarchuk, K. A., Lomonosov, A. M. Atmospheric Electric field as a Source of Ionospheric Variability. *Physics-Uspekhi,* **41**, No 5, 515-522, 1998

Pulinets, S. A., Benson, R. F. Radio-Frequency Sounders in Space, Review of Radio Science, ed. by W. Ross Stone, Oxford University Press, Chapter 28, 711-733, 1999

Pulinets, S. A., Boyarchuk, K. A., Hegai, V. V., Kim, V. P., Lomonosov, A. M. Quasielectrostatic Model of Atmosphere-Thermosphere-Ionosphere Coupling. *Adv. Space Res.*, **26**, 1209-1218, 2000

Roble, R. G., Tzur, I. The Global Atmospheric-Electrical Circuit. In The Earth's Electrical Environment, Studies in Geophysics series, National Academy Press, Washington D.C., 206-231, 1986

Schlegel, K., Diendorfer, G., Thern, S., Schmidt, M. Thunderstorms, Lightning and solar activity – Middle Europe. *J. Atm. Sol.-Terr. Phys.*, **63**, 1705-1713, 2001

Science of Space Environment. Ondoh, T., Marubashi, K. eds., Ohmsha Press, IOS Press, 94-95, 2000

**Figure Captions**

Fig. 1. The model (CCIR) global distribution of the critical frequency for July 1980 for the fixed local time 05 h LT (top panel) and global distribution of calculated ionosphere potential difference at the height 105 km (in Volts) along constant conductivity surface [*Roble and Tzur*, 1986] (bottom panel)

Fig. 2. Intercosmos-19 topside sounder derived global distribution of the critical frequency for July 1980 fixed local time 05:15 h LT (top panel) and the global distribution of the thunderstorm activity for July 1999 registered by the Optical Transient Detector device [*http://thunder.nsstc.nasa.gov/data/OTDsummaries/ (Optical Transient Detector)*] (bottom panel)

Fig. 3. Intercosmos-19 topside sounder derived global distribution of the critical frequency for November 1980 fixed local time 05:15 h LT (top panel) and the global distribution of the thunderstorm activity for November 1999 registered by the Optical Transient Detector device [*http://thunder.nsstc.nasa.gov/data/OTDsummaries/ (Optical Transient Detector)*] (bottom panel)

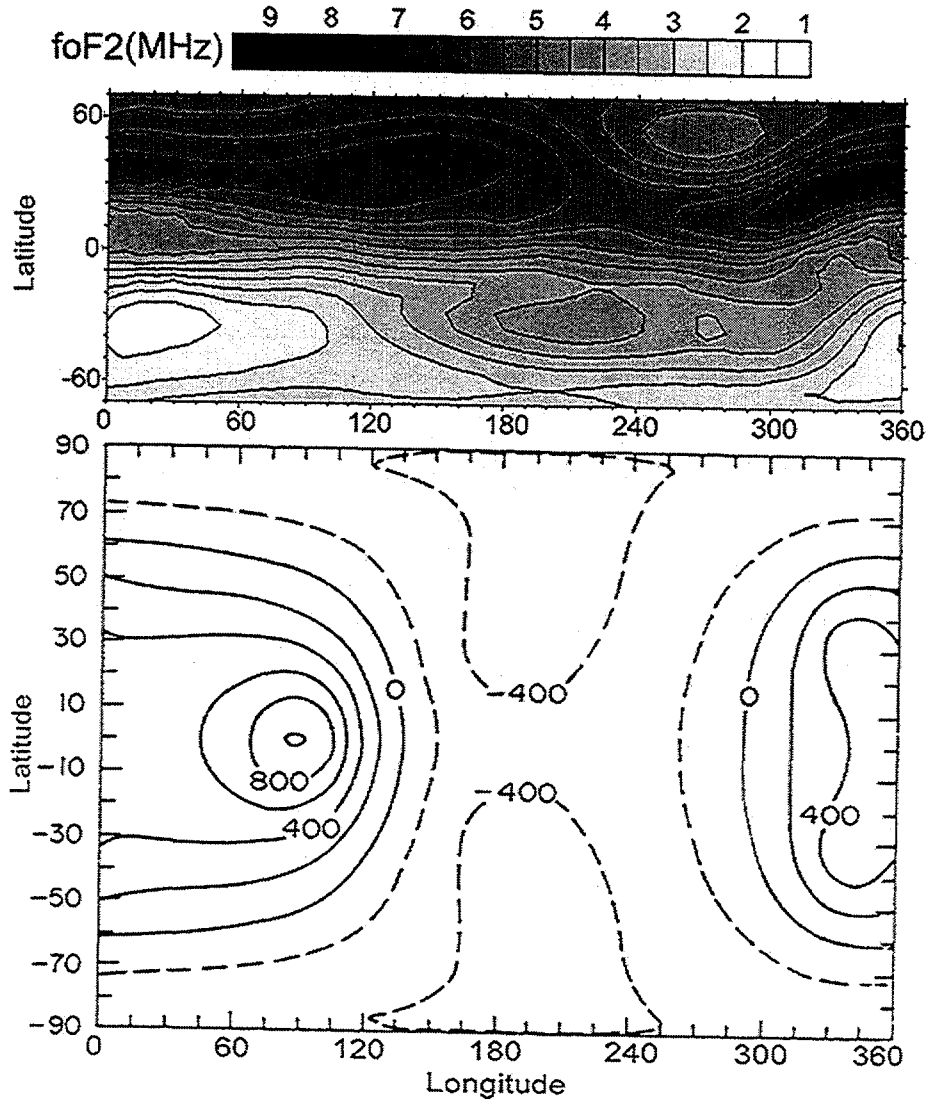
foF2(MHz)
9 8 7 6 5 4 3 2 1
60
0
-60
Latitude
0 60 120 180 240 300 360
90
70
50
30
10
-10
-30
-50
-70
-90
Latitude
800
400
0
-400
-400
0
400
0 60 120 180 240 300 360
Longitude

Fig. 1

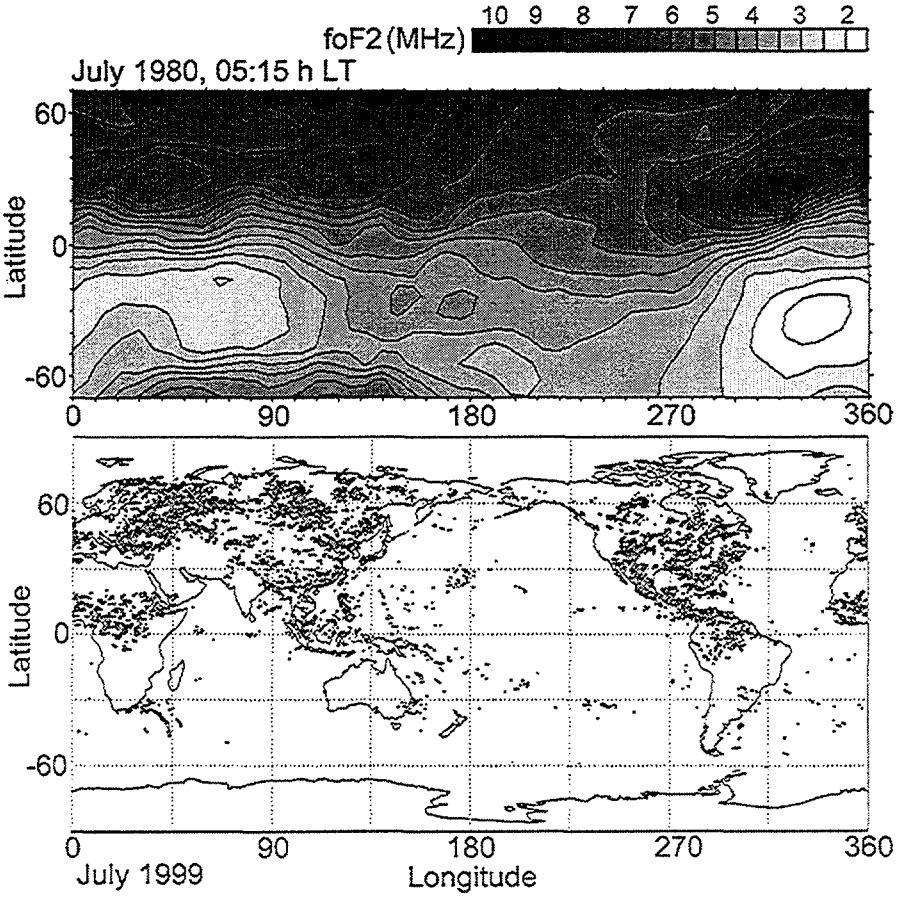
foF2 (MHz)
10 9 8 7 6 5 4 3 2
July 1980, 05:15 h LT
60
0
-60
Latitude
0
90
180
270
360
60
0
-60
Latitude
0
90
180
270
360
July 1999
Longitude

Fig. 2

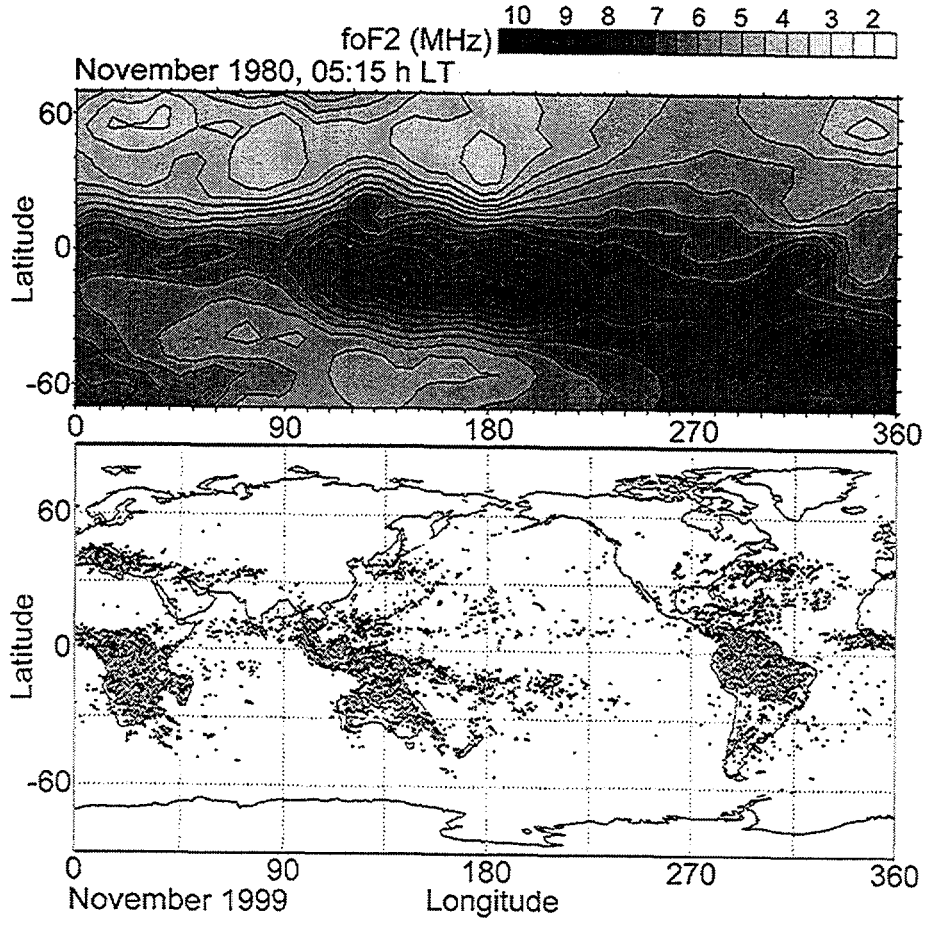
10 9 8 7 6 5 4 3 2
foF2 (MHz)
November 1980, 05:15 h LT
60
0
-60
Latitude
0
90
180
270
360
60
0
-60
Latitude
0
90
180
270
360
November 1999
Longitude

Fig. 3